Preferential solvation of thiophene and furan-2-carboxaldehyde phenylhydrazone derivatives in DMSO-water and DMSO-n-octanol mixtures

ARTICLE *in* SPECTROCHIMICA ACTA PART A MOLECULAR AND BIOMOLECULAR SPECTROSCOPY · NOVEMBER 2012

Impact Factor: 2.35 · DOI: 10.1016/j.saa.2012.10.057 · Source: PubMed

6 AUTHORS, INCLUDING:

Ysaías J. Alvarado
Venezuelan Institute for Scientific Research
49 PUBLICATIONS **491** CITATIONS
SEE PROFILE

Miguel Morales-Toyo
University of Zulia
4 PUBLICATIONS **9** CITATIONS
SEE PROFILE

Jelem Restrepo
Venezuelan Institute for Scientific Research
16 PUBLICATIONS **57** CITATIONS
SEE PROFILE

Spectrochimica Acta Part A: Molecular and Biomolecular Spectroscopy 103 (2012) 361–367

Contents lists available at SciVerse ScienceDirect

Spectrochimica Acta Part A: Molecular and Biomolecular Spectroscopy

journal homepage: www.elsevier.com/locate/saa

Preferential solvation of thiophene and furan-2-carboxaldehyde phenylhydrazone derivatives in DMSO–water and DMSO–*n*-octanol mixtures

Ysaías J. Alvarado [a,1,3,*], Alfonso Ballestas-Barrientos [a,3], Néstor Cubillán [b,2,*], Miguel Morales-Toyo [a,3], Jelem Restrepo [a,3], Gladys Ferrer-Amado [a,3]

[a] *Laboratorio de Caracterización Molecular y Biomolecular (LCMB), Departamento de Investigación en Tecnología de los Materiales y del Ambiente (DITeMA), Instituto Venezolano de Investigaciones Científicas (IVIC), Avenida 74 con calle 14A, Maracaibo, Edo. Zulia, Bolivarian Republic of Venezuela*

[b] *Laboratorio de Electrónica Molecular (LEM), Departamento de Química, Facultad Experimental de Ciencias, La Universidad del Zulia, Ap. 526, Grano de Oro, Módulo No. 2, Maracaibo, Estado Zulia, Bolivarian Republic of Venezuela*

HIGHLIGHTS

- We have studied preferential solvation (PS) by UV–Vis spectroscopy and TDDFT.
- The electron density moves from phenyl to heterocycle when there are no NO_2 groups.
- In the rest, the electron density moves from heterocycle to NO_2 groups.
- There is PS in DMSO–H_2O with a DMSO-rich cybotactic region for $x_{DMSO} > 0.5$.
- No PS was found in DMSO-1-octanol mixtures.

GRAPHICAL ABSTRACT

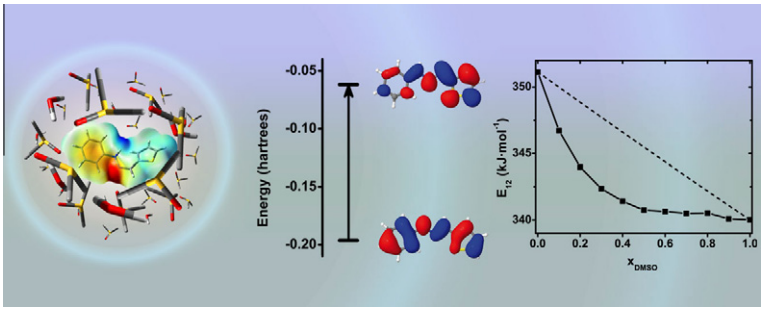

ARTICLE INFO

Article history:
Received 6 September 2012
Received in revised form 21 October 2012
Accepted 25 October 2012
Available online 7 November 2012

Keywords:
Phenylhydrazones
Preferential solvation
DMSO–water mixture
DMSO–*n*-octanol mixture
Electronic spectroscopy

ABSTRACT

The preferential solvation of thiophene- and furan-2-carboxaldehyde phenylhydrazone derivatives in DMSO–water and DMSO–*n*-octanol mixtures has been studied using visible absorption spectroscopy with a previous characterization of the electronic transitions by Time-Dependent Density Functional Theory (TDDFT) and solvatochromic study in several solvents with different hydrogen-bond donor capacity. The results indicate that the phenylhydrazones are preferentially solvated by clusters of DMSO–water existing in the solvent mixture and the dielectric enrichment as preferential solvation mechanism was discarded. A relation between local DMSO concentration with nitro groups and the electronegativity of the heteroatom of the five-membered ring was found. For DMSO–1-octanol mixtures, the results showed no preferential solvation.

Introduction

Phenylhydrazone derivatives have proved to be relevant molecules due to their potential medical applications [1–4]. Morgan and co-workers have proposed that the presence of both a nitro group in the *ortho*-position and hydrazone bridge seems to be an important condition for interactions with surface tumor markers [2]. Recently, we have described the relationship between the DNA-phenylhydrazone association constant and the number of nitro

* Corresponding authors. Tel.: +58 261 3231793 (Y.J. Alvarado), +58 261 6118413 (N. Cubillán).
E-mail addresses: yalvaradofec@yahoo.com, yalvarad@ivic.gob.ve (Y.J. Alvarado), ncubillan@fec.luz.edu.ve (N. Cubillán).
[1] Experimental section.
[2] Computational section.
[3] Tel.: +58 261 3231793.

1386-1425/$ - see front matter © 2012 Elsevier B.V. All rights reserved.
http://dx.doi.org/10.1016/j.saa.2012.10.057

groups on the phenyl moiety with the antiproliferative activity on breast tumor line MDA231 and hydrophobicity [5]. Theoretical and experimental studies have also shown that the hydrophobic effect is the major driving force involved in the binding of drugs to their receptor targets [6,7]. Nevertheless, the information about the chemical process of hydrazone compounds in solution is quite scarce [8–11].

In pharmacological studies, water and 1-octanol are currently used to simulate hydrophilic and hydrophobic medium respectively. The solubility measurements in these solvents give information about transport and binding of drugs. If the solute, drug candidate, is hydrophobic then it is necessary to use of a co-solvent in order to improve their solubility in aqueous medium. Primary among these co-solvents is DMSO, which is applied as a vehicle in drug therapy with a not exceeding concentration of 1% v/v [2,3,11].

In view of this it is necessary to obtain knowledge of the solvation behavior of these hydrophobic solutes in both aqueous and lipophilic (1-octanol) medium in presence of DMSO. Furthermore, it is also important to evaluate the role of this co-solvent in the nature of the solute–solvent and solvent–solvent interactions. The information above is necessary to explain the diffusion in cellular environments as well as the interpretation of pharmacokinetics and pharmacodynamics.

These considerations prompted us to inquire into the solvation of thiophene- and furan-2-carboxaldehyde phenylhydrazone, 4-phenylhydrazone and 2,4-dinitrophenylhydrazone derivatives (henceforth referred as PHF, PHT, NHF, NHT, DHF and DHT, respectively, as described in Fig. 1) in binary mixtures of DMSO–water and DMSO–*n*-octanol. This study was performed in three stages: First, a characterization of the electronic transitions with Time Dependent Density Functional Theory (TDDFT); second, an evaluation of the solvatochromism in several pure solvents with different hydrogen-bond donor capacity and, third, the preferential solvation in the above mentioned binary mixtures through visible absorption spectroscopy. Preferential solvation was discussed in terms of the two-stage model proposed by Chaterjee and Bagchi [12].

Computational studies

All molecular geometries were optimized with Cs symmetry constrains at Density Functional Theory (DFT) level using the hybrid functional B3LYP and 6-311++G(3d,3p) basis set. Time-Dependent Density Functional Theory (TDDFT) was used to evaluate electronic transitions at the experimental working range of wavelength (300–600 nm). All DFT and TDDFT calculations were achieved with Gaussian03W software [13]. Structures and orbitals were visualized with Jmol [14]. The partial density of states (PDOS) and the analysis of electronic transitions were obtained with GaussSum 2.2 [15].

Experimental

Phenylhydrazone derivatives mentioned above were synthesized via condensation of phenylhydrazine (98%, Merck), 4-nitrophenylhydrazine (99%, Merck) and 2,4-dinitrophenylhydrazine (99%, Merck) with the corresponding furan-2- (99%, Sigma–Aldrich) and thiophene-2-carboxaldehyde (98%, Sigma–Aldrich) following the methodology previously reported by us [9]. Organic solvents were obtained in the purest form available (HPLC grade), used without further purification and stored over molecular sieve: dimethyl sulfoxide (Sigma–Aldrich), methanol (Merck), propan-2-ol (Merck) and octan-1-ol (Merck). Doubly distilled and Deionized water was used throughout the experiments. DMSO–water and DMSO–*n*-octanol mixtures were prepared by carefully mixing the components until getting the desired mole fraction. DMSO was considered as the component 1 of the binary mixtures. The molar concentration of phenylhydrazone derivative (solute) in neat solvents, DMSO–water and DMSO–*n*-octanol mixtures was ranged between 10^{-4} and 10^{-5} mol dm^{-3} for solvatochromism and preferential solvation studies.

UV–Vis spectra were recorded on a Shimadzu Model UV-3101PC spectrometer using 1-cm quartz cells, except in pure water measurements in which a 4-cm cell was used due to the low water solubility of the solutes in order to reduce the signal-to-noise ratio. The temperature was kept constant at 293.15 K with a Peltier effect-based thermostatic unit Shimadzu CPS-260 and the working wavelength range was set between 300 and 600 nm. In order to check the reproducibility, the maximum absorption wavelength (λ^{max}) was taken at least five times in a particular solvent and solvent mixture, obtaining ±0.2 nm of precision. The energy of maximum absorption (E_{12}) was calculated from λ^{max} through the equation:

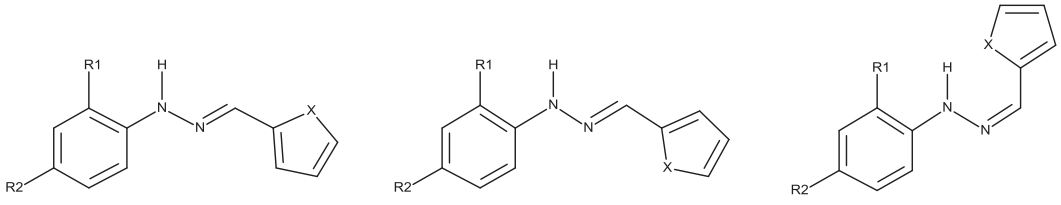

1 2 3

X	R1	R2	Abbrev.	IUPAC Name
O	H	H	PHF	1-(furan-2-ylmethylene)-2-phenylhydrazine
S	H	H	PHT	1-(thiophen-2-ylmethylene)-2-phenylhydrazine
O	H	NO_2	NHF	1-(furan-2-ylmethylene)-2-(4-nitrophenyl)hydrazine
S	H	NO_2	NHT	1-(thiophen-2-ylmethylene)-2-(4-nitrophenyl)hydrazine
O	NO_2	NO_2	DHF	1-(furan-2-ylmethylene)-2-(2,4-dinitrophenyl)hydrazine
S	NO_2	NO_2	DHF	1-(thiophen-2-ylmethylene)-2-(2,4-dinitrophenyl)hydrazine

Fig. 1. Referential structure, IUPAC name and abbreviations of the three low-energy isomers of phenylhydrazones of furan and thiophene under study.

$$E_{12} = \frac{hc}{\lambda^{max}} \quad (1)$$

where h is the Planck constant and, c is the speed of light. This equation is obtained by substituting frequency of light (ν) in the Planck–Einstein equation, $E = h\nu$ [16,17], by the universally accepted $\lambda\nu = c$ relation.

The refractive index of both pure solvent and mixed solvents at 657.7 nm were measured with a high resolution spectroscopic refractometer (Abbemat WR-MW, Anton-Paar) at 293.15 K.

Results and discussion

Prior to the preferential solvation analysis, calculations of the electronic structure and the orbital nature of transitions were carried out for the molecules of Fig. 1. Hence, we have performed DFT calculations considering the three low-energy isomers that possibly coexist in solution. These isomers were built based on rotations of the imine bond and the relative position of the heteroatom of the heterocycle, see Fig. 1. Details of the DFT results of energy, dipole moment, and HOMO–LUMO energies of each isomer are presented in Table SM1 of the Supplementary Material.

For furan-based derivatives, the DFT results reveal that the isomer 3 is the most-stable conformer, followed by isomer 1 with a difference of 3.7 kJ mol^{-1} with respect to the previous one. Nonetheless, crystallographic data for the acetyl-furan phenylhydrazone derivative, disclose that the isomer 1 exists exclusively in solid phase [18]. In the case of thiophene phenylhydrazone derivatives, the lowest energy isomer corresponds with the second structure, in agreement with the crystal structure of DHT as reported by Yin et al. [19].

The TDDFT results of the six phenylhydrazones are shown in Table 1, where λ, f and MO are the wavelength of electronic transitions at the working range, oscillator strength and the molecular orbital contributions for each excited state. The first band of these molecules is associated to the HOMO → LUMO transition with a contribution of around 80%. For the phenylhydrazone and *p*-nitrophenylhydrazone derivatives this band corresponds with the transition involving the higher oscillator strength, whereas for 2,4-dinitrophenylhydrazone derivatives the HOMO → LUMO + 1 transition is responsible for the most-absorbing band.

Fig. 2 shows the molecular orbitals involved in the electronic transitions of these molecules. From this figure and the partial density of states study, we have elucidated the electron density changes occurring in the important molecular groups associated to electronic transitions: (a) For phenylhydrazones derivatives, the HOMO → LUMO transition results from the movement of charge density from phenyl ring to the heterocycle. In *p*-nitro compounds, excitation results in an electron density transfer from the heteroatom to the nitro group. Finally, for 2,4-dinitro derivatives, the electron density movement from heterocycle to the nitro group in *ortho* position results in the first transition (HOMO → LUMO), whereas the same charge density transfer to the nitro group in *para*-position gives rise to the second transition (HOMO → LUMO + 1).

After the characterization of the electronic transitions of phenylhydrazones and before developing the preferential solvation study of the phenyl-hydrazone derivatives, the solvatochromic shift was measured in several pure solvents changing their hydrogen-bond donor capability and polarity. Solvents involved in this study were water, methanol, propan-2-ol, octan-1-ol and DMSO. The derivatives studied here exhibited moderate solvatochromic shifts of their maximum of the longest-wavelength absorption band in some single solvents at 293.15 K (see Fig. 3). These results show that the position of the band of each solute is affected not only by the polarity of medium but also by the number of nitro moiety and heteroatom. In this figure, it can be seen that the position of the absorption band of PHT undergoes a bathochromic shift as the solvent's hydrogen-bond acceptor capability increases (water < methanol < propan-2-ol < octan-1-ol) [20]. Stolyarov et al., mentioned that bathocromic shifts results from H bond formation between the negative center of the solvent and the hydrogen of the amine nitrogen when the excitation involves a decrease of the charge density in the amine nitrogen participating in such interaction [21], see Fig. 2.

For binary mixtures, DMSO–water and DMSO–*n*-octanol, it is necessary to mention the chemical forces involved in the mixing

Table 1
Time dependent DFT results of electronic transitions of phenylhydrazones of furan and thiophene.

	λ^{max} (nm)	λ (nm)	*f*	MO	λ (nm)	*f*	MO	λ (nm)	*f*	MO
			1			**2**			**3**	
PHF	351.4	352.3	0.7607	H → L (79%)	346.0	0.7508	H → L (79%)	351.6	0.6330	H → L (79%)
NHF	425.5	395.2	0.8152	H → L (85%)	389.9	0.8156	H → L (84%)	382.3	0.8184	H → L (84%)
	330.0	327.2	0.1995	H → L + 1 (78%)	322.5	0.2089	H → L + 1 (77%)	321.2	0.1069	H → L + 1 (80%)
				H-1 → L(8%)			H-1 → L (9%)			H-1 → L (8%)
DHF		459.5	0.1496	H → L (85%)	454.5	0.1494	H → L (85%)	442.7	0.0857	H → L (87%)
	406.0	394.4	0.6899	H → L + 1 (84%)	388.5	0.6942	H → L + 1 (84%)	381.3	0.6199	H → L + 1 (84%)
		325.1	0.116	H-1 → L (45%)	320.9	0.0906	H-1 → L (55%)	317.8	0.0404	H-1 → L (63%)
				H → L + 2 (48%)			H → L + 2 (39%)			H → L + 2 (33%)
	302.3	310.5	0.1163	H-1 → L (45%)	306.7	0.1449	H-1 → L (35%)	303.1	0.1311	H-1 → L (27%)
				H-1 → L + 1 (11%)			H-1 → L + 1 (12%)			H-1 → L + 1 (15%)
				H → L + 2 (30%)			H → L + 2 (37%)			H → L + 2 (42%)
PHT	364.6	364.3	0.7171	H → L (80%)	366.6	0.6333	H → L (81%)	362.2	0.5588	H → L (82%)
NHT	429.1	394.1	0.8901	H → L (84%)	393.1	0.851	H → L (84%)	381.7	0.8337	H → L (84%)
	338.9	332.4	0.1154	H → L + 1 (81%)	333.3	0.0858	H → L + 1 (82%)	325.2	0.0473	H → L + 1 (83%)
				H-1 → L (7%)			H-1 → L (5%)			H-1 → L (6%)
DHT		453.5	0.1654	H → L (85%)	451.9	0.1669	H → L (85%)	438.3	0.085	H → L (88%)
	409.3	391.6	0.7349	H → L + 1 (84%)	390.3	0.698	H → L + 1 (84%)	379.5	0.633	H → L + 1 (86%)
		326.2	0.0971	H-1 → L (20%)	326.4	0.0811	H-1 → L (14%)	318.4	0.0321	H-1 → L (56%)
				H → L + 2 (67%)			H → L + 2 (70%)			H → L + 2 (37%)
		308.6	0.0483	H-1 → L (61%)	310.5	0.0117	H-1 → L (71%)	305.6	0.0999	H-1 → L (38%)
				H → L + 2 (14%)			H → L + 2 (9%)			H → L + 2 (37%)
				H-2 → L (6%)			H-2 → L (7%)			H-2 → L (7%)

λ^{max}: experimental wavelength of the electronic absorption band maxima measured in DMSO; λ: wavelength of electronic excitations calculated at TDDFT/B3LYP/6-311++G(3d,3p) level of theory; *f*: oscillator strength calculated with TDDFT; MO: molecular orbital; H: HOMO; L: LUMO.

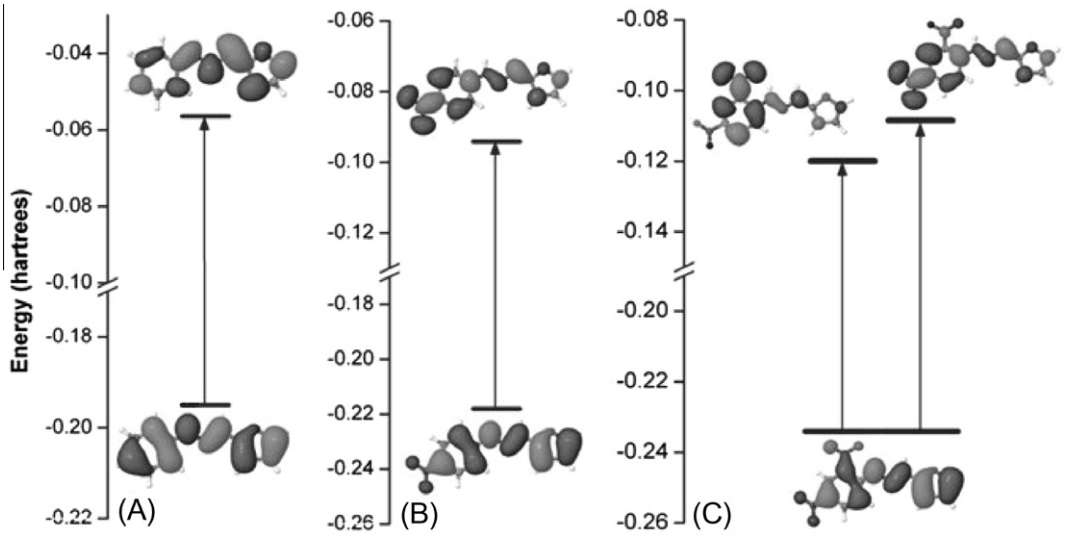

Fig. 2. Orbital nature of electronic transitions of: (A) phenylhydrazones, (B) 4-nitro-phenylhydrazones and (C) 2,4-dinitro-phenylhydrazones.

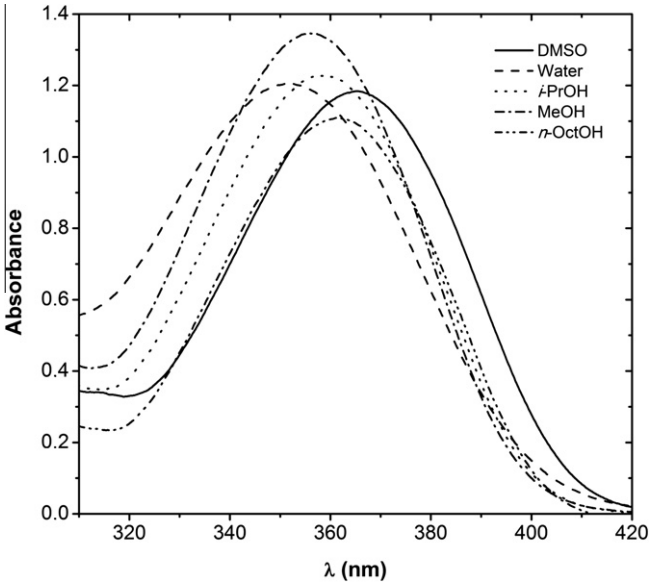

Fig. 3. Absorption spectra of PHT in neat solvents.

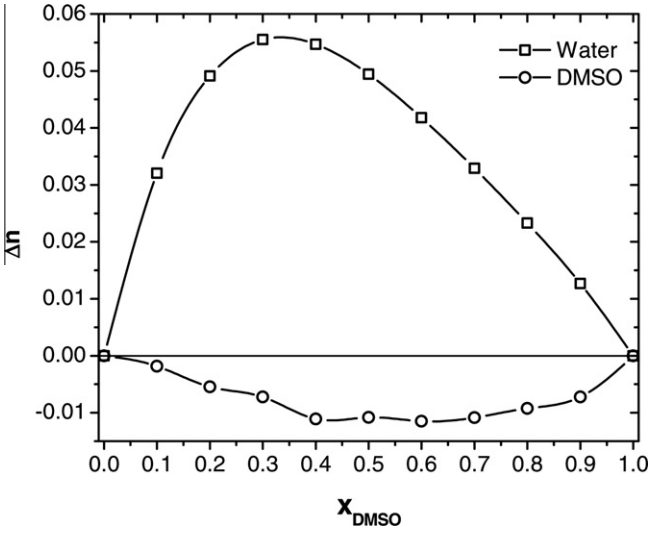

Fig. 4. Excess refractive index for DMSO–water and DMSO–*n*-octanol binary mixtures.

processes. DMSO with water mix through a clustering phenomenon via formation of hydrogen bonds between S═O and OH groups. This process entails breaking both hydrogen bonds network of water and dipolar clusters of DMSO [22–24]. On the other hand, these interactions between DMSO and normal alkanols in solution are not favored and decrease with the increasing of the chain length of the alkanol [25,26]. Consequently, the solvent–solvent dispersion forces are operative in these systems and tend to dominate in the DMSO–alkanols mixtures and in particular in DMSO–1-octanol mixtures [25,26]. In fact, as can be seen in Fig. 4, the values of the excess refractive index obtained in this work at 657.7 nm, 293.15 K and 1 atm for the binary system DMSO–H_2O exhibits positive values whereas the values for DMSO–1-octanol mixture are negatives over the whole composition range. The positive values with the increasing mole fraction of DMSO are attributed to the increase in the electronic polarization of the system due to the formation of dipolar DMSO–water clusters, while the negative values are attributed to the decrease in the strength of the interaction between DMSO and 1-octanol via hydrogen bonding.

In the case of DMSO–water mixtures a red shift of the most-absorbing band was observed as the DMSO mole fraction increases without isobestic point. Also, no change in the bandwidth and shape with the mixture composition and solute concentration at the working range was evidenced (see Fig. 5). Both characteristics, confirm the absence of solute–solute and solute–solvent specific interactions. A revision of the total wavelength shift [$\lambda^{max}(H_2O)$-$\lambda^{max}(DMSO)$] for the different compounds reveals a low variation for *p*-nitrophenylhydrazones (~4 nm), followed by phenylhydrazones (approx. 8 nm) and finally 2,4-dinitrophenylhydrazones (~12 nm). Interestingly, the smallest variation observed in this work is higher than those recently reported for hydrophobic 1,4-dimethoxy-3-methylanthracene-9,10-dione derivative in some mixed aprotic solvents [27].

In Table 2 the values of the energy of maximum absorption (E_{12}) expressed in kJ mol^{-1} are listed for each system at different compositions at 293.15 K and 1 atm. For DMSO–water mixtures, E_{12} is a nonlinear function of the mole fraction of DMSO (x_1) and the positive deviation from linearity indicates that the solvation shell of each solute has a higher concentration of DMSO than in the bulk (see Fig. 6).

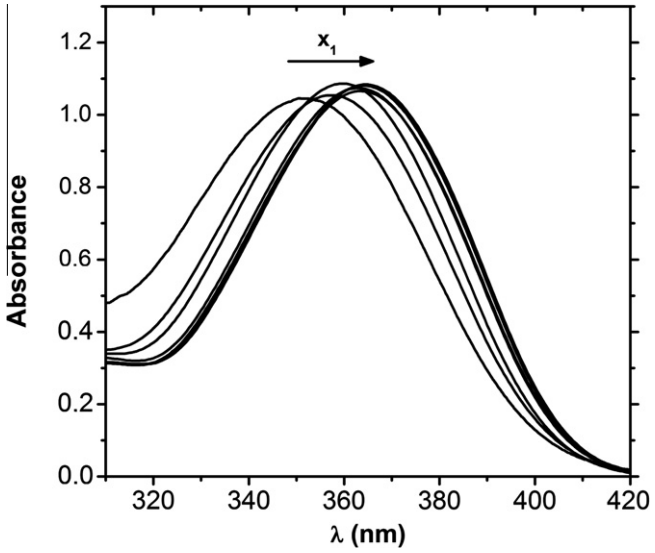

Fig. 5. Absorption spectra of PHT in DMSO–water binary mixtures.

The deviation from ideality was quantitatively estimated using the Ben-Naim definition [28]. According to this, the local (i.e. cybotactic region or solvation shell) concentration (x_1^L) of DMSO in the scale of mole fraction is given by

$$x_1^L - x_1 = \frac{E_{12} - x_1E_1 - x_2E_2}{E_1 - E_2} \quad (2)$$

where E_1 and E_2 are the electronic transition energies in pure DMSO and water, respectively. The values obtained for this parameter in each case can be seen in Table 2.

A cursory look of this table reveals that for all compounds in DMSO–water mixtures, the local composition of DMSO (x_1^L) was greater than the bulk concentration of the same cosolvent in the whole mole fraction range. Henceforth, for a mole fraction of DMSO in the bulk (x_1) of 0.2 the values of x_1^L were greater than 0.55 increasing with the number of nitro group in the phenyl ring. However, for furan derivatives the order was DHF > PHF > NHF revealing an anomalous behavior for *p*-nitro compound. In all cases, the values at $x_1 = 0.5$ shows that the cybotactic region consists practically of DMSO. Macdonald and Hyde found that for solutions with mole fraction of DMSO in water greater than 0.5, the structure of this binary system varies little with respect to pure DMSO [29]. However other works have shown that the solvation of solutes in DMSO–water mixtures occurs by interaction with solvent clusters rather than with individual solvent components [23,24,30].

It is interesting to observe that all solutes are preferentially solvated by the aprotic solvent of the binary mixtures. These results allow us to suggest that the excited state is further stabilized by DMSO or DMSO–H_2O aggregates. These DMSO–H_2O clusters can preferentially solvate hydrophobic solutes orientating the methyl groups of DMSO towards the hydrophobic solute in order to offer a hydrophobic microenvironment at mole fractions of DMSO $x_1 > 0.2$ [30]. In pure water or water rich region the blue-shift can be due to the stabilization of the lone pairs on atoms (e.g. O, N, S) or negative charges of derivatives in the dipolar field of the group of water or by means of hydrogen bonding in the ground state [20].

The results of the solvatochromic behavior of thiophene and furan phenylhydrazone derivatives in the binary mixture DMSO–1-octanol are shown in Table 2. In all cases the energy of maximum

Table 2
Preferential solvation parameters for phenylhydrazone derivatives in DMSO–H_2O and DMSO–*n*-octanol binary mixtures.

DMSO–H_2O				DMSO–*n*-octanol		
x_1	λ^{max} (nm)	E_{12} (kJ mol^{-1})	x_1^L	λ^{max} (nm)	E_{12} (kJ mol^{-1})	x_1^L
PHT						
0.0	352.0	339.5	0.000	360.5	331.5	0.000
0.1	357.5	334.3	0.445	361.0	331.0	0.126
0.2	359.8	332.2	0.623	361.4	330.6	0.231
0.3	361.2	330.9	0.734	361.8	330.3	0.315
0.4	362.3	329.8	0.825	362.1	330.0	0.398
0.5	363.0	329.2	0.877	362.7	329.5	0.544
0.6	363.5	328.8	0.915	363.0	329.2	0.628
0.7	364.0	328.3	0.954	363.3	329.0	0.690
0.8	364.3	328.0	0.977	363.8	328.5	0.814
0.9	364.5	327.9	0.992	364.2	328.2	0.918
1.0	364.6	327.8	1.000	364.5	327.9	1.000
PHF						
0.0	340.3	351.1	0.000	347.5	343.9	0.000
0.1	344.7	346.7	0.397	348.0	343.4	0.144
0.2	347.4	344.0	0.643	348.4	343.0	0.264
0.3	349.1	342.4	0.789	348.6	342.8	0.311
0.4	350.0	341.4	0.873	349.0	342.4	0.431
0.5	350.7	340.8	0.935	349.3	342.1	0.525
0.6	350.8	340.7	0.943	349.5	341.9	0.574
0.7	351.0	340.5	0.956	349.9	341.5	0.693
0.8	350.9	340.5	0.954	350.5	340.9	0.858
0.9	351.4	340.1	0.993	350.7	340.8	0.906
1.0	351.4	340.0	1.000	351.0	340.5	1.000
NHT						
0.0	425.0	281.2	0.000	413.2	289.2	0.000
0.1	426.6	280.1	0.390	415.1	287.9	0.126
0.2	428.0	279.2	0.737	416.8	286.7	0.238
0.3	428.3	279.0	0.797	418.9	285.3	0.369
0.4	428.5	278.9	0.858	420.4	284.3	0.466
0.5	428.5	278.9	0.858	422.0	283.2	0.567
0.6	428.5	278.9	0.858	423.3	282.3	0.645
0.7	428.5	278.9	0.858	424.7	281.4	0.734
0.8	428.8	278.7	0.939	426.0	280.5	0.816
0.9	428.8	278.7	0.939	427.4	279.6	0.903
1.0	429.1	278.5	1.000	429.0	278.6	1.000
NHF						
0.0	421.0	283.9	0.000	405.8	294.5	0.000
0.1	422.1	283.1	0.243	409.1	292.1	0.172
0.2	423.5	282.2	0.558	411.0	290.8	0.272
0.3	424.4	281.6	0.761	414.0	288.7	0.427
0.4	424.7	281.4	0.816	415.8	287.43	0.516
0.5	425.0	281.2	0.890	417.5	286.2	0.605
0.6	424.8	281.3	0.835	419.6	284.8	0.709
0.7	425.0	281.2	0.890	420.4	284.3	0.750
0.8	425.1	281.1	0.912	422.0	283.2	0.829
0.9	425.2	281.1	0.927	423.5	282.2	0.903
1.0	425.5	280.9	1.000	425.5	280.9	1.000
DHT						
0.0	388.5	307.6	0.000	390.0	306.4	0.000
0.1	400.1	298.7	0.569	393.0	304.1	0.156
0.2	406.1	294.3	0.855	394.9	302.6	0.254
0.3	406.1	294.3	0.854	396.8	301.2	0.347
0.4	406.8	293.8	0.885	398.3	300.1	0.423
0.5	407.4	293.3	0.916	399.6	299.1	0.490
0.6	407.7	293.1	0.927	402.7	296.8	0.642
0.7	407.9	293.0	0.939	403.2	296.4	0.667
0.8	408.3	292.7	0.954	404.5	295.4	0.732
0.9	409.0	292.2	0.989	407.5	293.3	0.877
1.0	409.3	292.0	1.000	410.1	291.4	1.000
DHF						
0.0	388.5	307.6	0.000	388.0	308.0	0.000
0.1	400.0	298.8	0.667	390.9	305.7	0.166
0.2	401.7	297.5	0.764	392.7	304.3	0.265
0.3	402.6	296.8	0.813	394.5	302.9	0.370
0.4	403.6	296.1	0.868	395.5	302.2	0.421
0.5	404.7	295.3	0.929	397.5	300.7	0.532
0.6	405.0	295.1	0.945	398.8	299.6	0.606

(*continued on next page*)

Table 2 (*continued*)

DMSO–H_2O				DMSO–*n*-octanol		
x_1	λ^{max} (nm)	E_{12} (kJ mol^{-1})	x_1^L	λ^{max} (nm)	E_{12} (kJ mol^{-1})	x_1^L
0.7	405.8	294.5	0.987	402.0	297.3	0.777
0.8	405.8	294.5	0.987	403.0	296.5	0.831
0.9	405.7	294.6	0.984	405.3	294.8	0.954
1.0	406.0	294.3	1.000	406.2	294.2	1.000

x_1: bulk mole fraction of DMSO; λ^{max}: maximum absorption wavelength (nm); E_{12}: energy of maximum absorption (kJ mol^{-1}); x_1^L: local mole fraction of DMSO.

absorption (E_{12}) has shown relatively small deviations from linearity (see Fig. 7).

These results indicate that the microenvironment (solvation shell) of each solute in this mixture is the same as the bulk composition. This can be rationalized in terms of the similar solute–DMSO and solute–1-octanol interactions (nonspecific components of van der Waals) and not H-bonds occurring in the solvation shell. It may be assumed that both solute–alcohol and solute–DMSO dispersion interactions are similar in magnitude and consist practically in the fitting of 1-octanol alkyl chains and methyl groups of DMSO to the surface of the hydrophobic core of the solute molecules. It could also be implied that nonspecific interactions between solvent components (DMSO and 1-octanol) in the local region are similar to those in the bulk.

According to these results the factor responsible for the nonlinear behavior of the transition band in the mixed solvents is the specific interaction of each solute with the DMSO–water aggregates rather than the DMSO or H_2O clusters itself. In consequence, the dielectric enrichment [20] – the solvation shell of solute is enriched in polar solvent from the bulk mole fraction – as solvation mechanism in these systems can be rejected.

On the other hand, Alvarado et al. [5,8] have established that the hydrophobicity and electronic polarizability of the phenylhydrazone derivatives increase with both the number of nitro group and atomic number of the heteroatom of the heterocycle. With this information, the dependence of local mole fraction of DMSO, x_1^L, obtained in this study with the number of nitro group and heteroatom is feasibly understood.

Conclusions

The results obtained indicate that the synthesized hydrophobic phenylhydrazone are preferentially solvated by clusters of DMSO–water existing in the solvent mixture. The dielectric enrichment as preferential solvation mechanism was discarded. The local DMSO concentration around of furan- and thiophene-2-carboxaldehyde phenylhydrazones was highly increased with the increment of nitro groups on the phenyl moiety and the electronegativity of the heteroatom of the five-membered ring. For DMSO–1-octanol mixtures, the results showed no preferential solvation of the solute by any of the components, and no difference between the cybotactic and bulk region was evidenced.

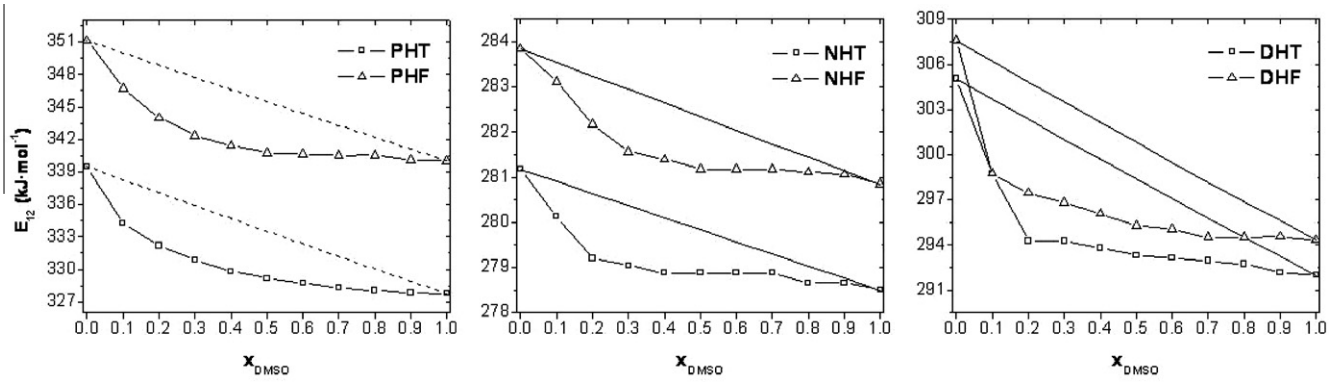

Fig. 6. Graphical representation of E_{12} of phenylhydrazone derivatives in DMSO–water binary solvent mixtures as a function of mole fraction of DMSO (x_1).

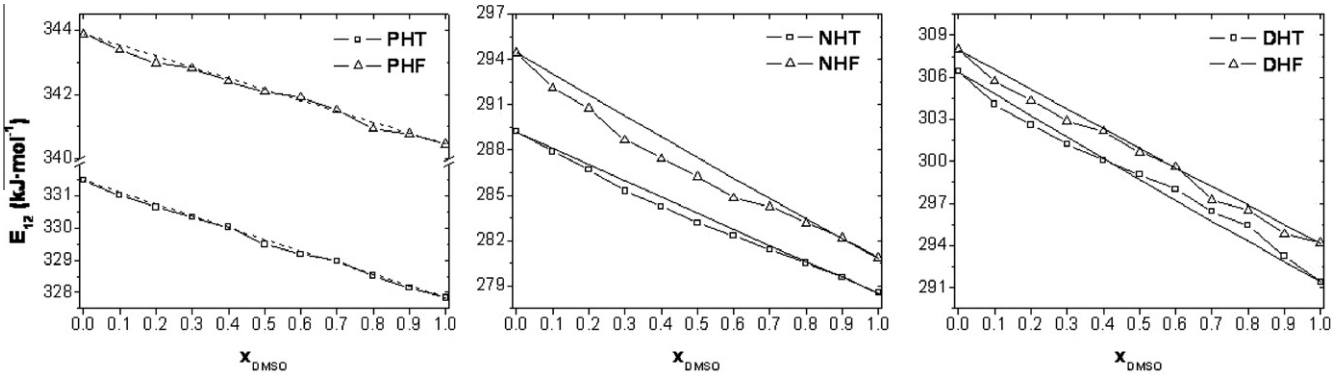

Fig. 7. Plot of E_{12} of phenylhydrazone derivatives in DMSO–*n*-octanol binary solvent mixtures as a function of mole fraction of DMSO (x_1).

Appendix A. Supplementary material

Supplementary data associated with this article can be found, in the online version, at http://dx.doi.org/10.1016/j.saa.2012.10.057.

References

[1] D.S. Kalinowski, D.R. Richardson, Pharmacol. Rev. 57 (2005) 547–583.
[2] L.R. Morgan, B.S. Jursic, C.L. Hooper, D.M. Neumann, K. Thangaraj, B. LeBlanc, Bioorg. Med. Chem. Lett. 12 (2002) 3407–3411.
[3] L.R. Morgan, K. Thangaraj, B. LeBlanc, A. Rodgers, L.T. Wolford, C.L. Hooper, D. Fan, B.S. Jursic, J. Med. Chem. 46 (2003) 4552–4563.
[4] S.K. Rollas, S.G., Molecules 12 (2007) 1910–1939.
[5] Y. Alvarado, J. Baricelli, J. Caldera-Luzardo, N. Cubillán, G. Ferrer-Amado, Y. Marrero-Ponce, V. Mancilla, M. Rocafull, J. Ojeda-Andara, L. Thomas, J. Vera-Villalobos, M. Morales-Toyo, J. Solution Chem. 40 (2011) 26–39.
[6] S. Miyamoto, P.A. Kollman, Proc. Natl. Acad. Sci. USA 90 (1993) 8402–8406.
[7] R. Patil, S. Das, A. Stanley, L. Yadav, A. Sudhakar, A.K. Varma, PLoS ONE 5 (2010) e12029.
[8] Y. Alvarado, M. Álvarez-Mon, J. Baricelli, J. Caldera-Luzardo, N. Cubillán, G. Ferrer-Amado, M. Hassanhi, Y. Marrero-Ponce, V. Mancilla, M. Rocafull, M. San Antonio-Sánchez, J. Ojeda-Andara, L. Thomas, J. Solution Chem. 39 (2010) 1099–1112.
[9] Y.J. Alvarado, J. Caldera-Luzardo, G. Ferrer-Amado, V. Mancilla-Labarca, E. Michelena, J. Solution Chem. 36 (2007) 1–11.
[10] S. Sagiraju, B.S. Jursic, Carbohyd. Res. 343 (2008) 1180–1190.
[11] N.C. Santos, J. Figueira-Coelho, J. Martins-Silva, C. Saldanha, Biochem. Pharmacol. 65 (2003) 1035–1041.
[12] P. Chatterjee, S. Bagchi, J. Phys. Chem. 95 (1991) 3311–3314.
[13] M.J. Frisch, G.W. Trucks, H.B. Schlegel, G.E. Scuseria, M.A. Robb, et al., Gaussian 03, Revision D.02. Gaussian, Inc., Wallingford CT, 2004.
[14] Jmol, An open-source Java viewer for chemical structures in 3D. <http://www.jmol.org/>.
[15] N.M. O'Boyle, A.L. Tenderholt, K.M. Langner, J. Comput. Chem. 29 (2008) 839–845.
[16] A. Einstein, Annalen der Physik 325 (1906) 199–206.
[17] M. Planck, Ann. der Physik 309 (1901) 553–563.
[18] S. Shan, Y.-L. Tian, S.-H. Wang, W.-L. Wang, Y.-L. Xu, Acta Crystallogr. E 64 (2008) o1153.
[19] Z.-g. Yin, H.-y. Qian, H.-p. Li, J. Hu, C.-x. Zhang, Acta Crystallogr. E 64 (2008) o2421.
[20] P. Suppan, N. Ghoneim, Solvatochromism, Royal Society of Chemistry, Fribourg, Switzerland, 1997.
[21] A.N. Stolyarov, B.I. Buzykin, Y.P. Kitaev, Russ. Chem. Bull. 26 (1977) 946–948.
[22] S.E. McLain, A.K. Soper, A. Luzar, J. Chem. Phys. 127 (2007) 174515.
[23] D.N. Shin, J.W. Wijnen, J.B.F.N. Engberts, A. Wakisaka, J. Phys. Chem. B 105 (2001) 6759–6762.
[24] D.N. Shin, J.W. Wijnen, J.B.F.N. Engberts, A. Wakisaka, J. Phys. Chem. B 106 (2002) 6014–6020.
[25] A. Ali, K. Tewari, A.K. Nain, V. Chakravortty, Phys. Chem. Liq. 38 (2000) 459–473.
[26] V. Syamala, K. Siva Kumar, P. Venkateswarlu, J. Mol. Liq. 136 (2007) 29–34.
[27] M. Umadevi, M.V. Kumari, M.S. Bharathi, P. Vanelle, T. Terme, Spectrochim. Acta, Part A 78 (2011) 122–127.
[28] A. Ben-Naim, Cell Biochem. Biophys. 12 (1988) 255–269.
[29] D.D. Macdonald, J.B. Hyne, Can. J. Chem. 49 (1971) 2636–2642.
[30] T. Bevilaqua, T.F. Gonçalves, C.d.G. Venturini, V.G. Machado, Spectrochim. Acta, Part A 65 (2006) 535–542.